

THE MAGNETIC STRUCTURES OF  $\text{DyNi}_2\text{Ge}_2$ Zahirul Islam<sup>a,1</sup>, C. Detlefs<sup>a,2</sup>, A.I. Goldman<sup>a</sup>, S.L. Bud'ko<sup>a</sup>, P.C. Canfield<sup>a</sup> and A. Zheludev<sup>b</sup><sup>a</sup> Ames Laboratory and Department of Physics and Astronomy, Iowa State University, Ames, Iowa, IA 50011, U.S.A.<sup>b</sup> Department of Physics, Brookhaven National Laboratory, Upton, New York, NY 11973, U.S.A.

(Received 21 July 1998; accepted 3 August 1998 by P. Burlet)

In this paper we report the results of neutron diffraction measurements of the magnetic structures of a single crystal of  $\text{DyNi}_2\text{Ge}_2$  in zero applied magnetic field. There are two distinct magnetic transitions in this material; one is from the paramagnetic phase to an *amplitude modulated* (AM) *antiferromagnetic* phase at the Néel temperature,  $T_N = 8.3 \pm 0.1$  K, and the other is at a lower temperature,  $T_1 = 3.1 \pm 0.2$  K, from this phase to an *equal moment* (EM) *antiferromagnetic* structure. The EM structure is described by a set of three wave vectors, namely,  $\tau_1 = (0 \ 0 \ \frac{3}{4})$ ,  $\tau_2 = (\frac{1}{2} \ \frac{1}{2} \ 0)$  and  $\tau_3 = (\frac{1}{2} \ \frac{1}{2} \ \frac{1}{2})$ . A weak third harmonic,  $\tau'_1 = (0 \ 0 \ \frac{1}{4})$ , related to  $\tau_1$ , also appears indicating that the magnetic structure is not purely sinusoidal. In this phase Dy moments have their full saturation value of  $\mu_s = 10 \mu_B$ . The AM phase is described by a single propagation vector  $\tau_1$ . In both the phases there is an ordered component of the Dy moments in the basal plane. The angle between the ordered Dy moments and the  $\hat{c}$  axis is estimated to be  $17^\circ \pm 6^\circ$  at 1.5 K. These results are consistent with the dc susceptibility as a function of temperature data which shows weak anisotropy and two transitions.

© 1998 Elsevier Science Ltd. All rights reserved.

Keywords: A. magnetically ordered materials, D. phase transitions, E. neutron scattering.

## 1. INTRODUCTION

In the study of the interplay between long range magnetic order and single-ion anisotropy in rare earth intermetallic compounds, tetragonal systems offer distinct advantages. Many of these systems are either uniaxial or planar in their anisotropic magnetic behaviors. This anisotropy is primarily determined by the crystal electric field (CEF) splittings of the Hund's rule ground state  $J$  multiplet which, in tetragonal systems, requires only a few parameters to be specified. The  $\text{RNi}_2\text{Ge}_2$  family is such a system. Its magnetic properties are similar to those of the  $\text{RNi}_2\text{Si}_2$  series which exhibits considerable magneto-crystalline anisotropy. [1] Until recently, however, bulk measurements on  $\text{RNi}_2\text{Ge}_2$

materials have been performed on polycrystalline samples where the valuable information about anisotropy was lost due to powder averaging. Recently, high quality single crystals of these materials have been grown in Ames Laboratory using a high-temperature-flux-growth [2] technique and their magnetic and electronic transport properties as a function of rare earth component have been studied in detail. [3]

As a part of this series-wide study we have carried out a complete determination of the zero field magnetic structures of  $\text{TbNi}_2\text{Ge}_2$  using both neutron diffraction and X-ray resonant exchange scattering (XRES) techniques. [4] In addition, XRES studies of  $\text{GdNi}_2\text{Ge}_2$  and  $\text{EuNi}_2\text{Ge}_2$  magnetic structures have also been performed which will be published elsewhere. [5] The present work is concerned with the zero field magnetic structures of another member of

<sup>1</sup> E-mail: zahirul@iastate.edu<sup>2</sup> Present Address: ESRF, Grenoble, France.

this family,  $\text{DyNi}_2\text{Ge}_2$ , which will provide a starting point for future investigations of the field induced structures mentioned below.

$\text{DyNi}_2\text{Ge}_2$  crystallizes in the body centered tetragonal  $\text{ThCr}_2\text{Si}_2$  structure [6] with space group  $I4/mmm$  (for details see Ref. [4]). The magnetic properties of this material have been studied by various groups. The ordering temperature of 11 K reported by earlier groups [7, 8] is considerably different than those found by André and co-workers who have carried out a detailed study on polycrystalline  $\text{DyNi}_2\text{Ge}_2$  sample. [9] They observed a paramagnetic to an antiferromagnetic phase transition at  $T_N = 7.5$  K in their susceptibility measurement. According to their powder neutron diffraction measurements, this transition takes place at 8.5 K. Using neutron diffraction methods on powder sample they found the ordered phase, at 1.4 K, to be an *incommensurate sinusoidally amplitude modulated* (AM) structure with propagation vector  $(0\ 0\ 0.788)$ . Further, they found that the ordered Dy moments form an angle of  $20^\circ$  with the  $\hat{c}$  axis. As shown below the transition temperatures and, the propagation vectors are significantly different in high quality single crystals.

High quality single crystals of  $\text{DyNi}_2\text{Ge}_2$  were grown at Ames Laboratory using a high-temperature-flux-growth technique. [2] X-ray powder diffraction pattern confirmed the room temperature structure to be of the  $\text{ThCr}_2\text{Si}_2$  type with no evidence of second phases. The anisotropic magnetization was measured using a Quantum Design MPMS-5 SQUID magnetometer which provides a temperature range of 1.8 K–350 K and a magnetic field upto 55 kG.

The neutron scattering measurements on a single crystal of  $\text{DyNi}_2\text{Ge}_2$  were carried out at the H4M spectrometer of High Flux Beam Reactor (HFBR) at Brookhaven National Laboratory. Neutrons with energies of 14.7 meV were used with collimator settings of  $40'-40'-80'$ -none. Pyrolytic graphite filters were used to eliminate second harmonic ( $\frac{\lambda}{2}$ ) contamination of the beam. No special preparation of the sample was necessary. The largest crystal of the same batch used for the magnetization measurements was chosen. The sample was closely a square plate with dimensions of  $7\text{ mm} \times 7\text{ mm} \times 1.5\text{ mm}$  and weighing about 300 mg.

## 2. MAGNETIZATION

The temperature dependence of the low field susceptibility with applied field parallel ( $H \parallel \hat{c}$ ) and perpendicular ( $H \perp \hat{c}$ ) to the  $\hat{c}$  axis was found to be anisotropic. From cusps in the susceptibility two transitions were identified, and are indicated in Fig. 1(a).

The paramagnetic to antiferromagnetic transition occurs at  $T_N = 8.2$  K. The second transition is at a lower temperature,  $T_1 = 3.2$  K. This is in contrast to previous susceptibility measurement [9] where only one transition at  $T_N = 7.5$  K was observed. This may be a consequence of polycrystalline averaging which often makes the lower transition less pronounced as was found to happen in  $\text{GdNi}_2\text{B}_2\text{C}$  (see Ref. [10]). In this material a second transition at 14 K (the Néel temperature is 20 K) due to the Gd spin reorientation was observed using XRES. [11] Such subtle transitions are particularly difficult to detect in a polycrystalline sample.

The magnetization as a function of field applied along the  $\hat{c}$  axis at 2 K (Fig. 1(b)) shows two metamagnetic transitions at 18 kG and 27 kG respectively. We believe that on further lowering of the temperature these transitions would become sharper (similar to data in Ref. [4]) with the appearance of at least one more transition approximately at 9 kG which is barely discernible at this temperature. Also since the moment does not acquire the full saturation value of  $10\ \mu_B$  up to 55 kG it is conceivable that there may be one or more metamagnetic transitions in higher fields. When the field is in the basal plane, however, the magnetization does not manifest any transitions.

This magnetic behavior is very similar to that of the isostructural  $\text{DyNi}_2\text{Si}_2$  compound. [12–14] This material has two magnetic phase transitions, at 3.4 K and 6 K, respectively. As in  $\text{DyNi}_2\text{Ge}_2$ , the anisotropy is not very strong. At 1.5 K, there are four metamagnetic transitions with field applied along the  $\hat{c}$  axis. [12] This behavior was found to be qualitatively like that of  $\text{TbNi}_2\text{Si}_2$ . [15] The zero field magnetic structures in these two materials were found also to be quite similar. [13, 16]

Interestingly, the magnetic behavior of  $\text{DyNi}_2\text{Ge}_2$  is also qualitatively similar to that of the neighboring member of the series,  $\text{TbNi}_2\text{Ge}_2$ , which exhibits two magnetic transitions, [3, 4] at  $T_N = 16.8$  K and  $T_1 = 9.3$  K, respectively, in zero field. The magnetization measurements on this material at 2 K with the field parallel to the  $\hat{c}$  axis shows a sequence of five metamagnetic transitions below 55 kG. Both the susceptibility and magnetization showed strong anisotropy with the  $\hat{c}$  axis as the easy axis of magnetization. Neutron and XRES measurements showed indeed the ordered moments are aligned with the  $\hat{c}$  axis. This material was shown to be a good candidate for the study of metamagnetic phase transitions and possibly “devil’s staircase” (see Ref. [17]) type behavior. In the case of  $\text{DyNi}_2\text{Ge}_2$  the anisotropy is not as strong as in  $\text{TbNi}_2\text{Ge}_2$ . This implies that there may be ordered component of Dy moments in the basal plane. Also,

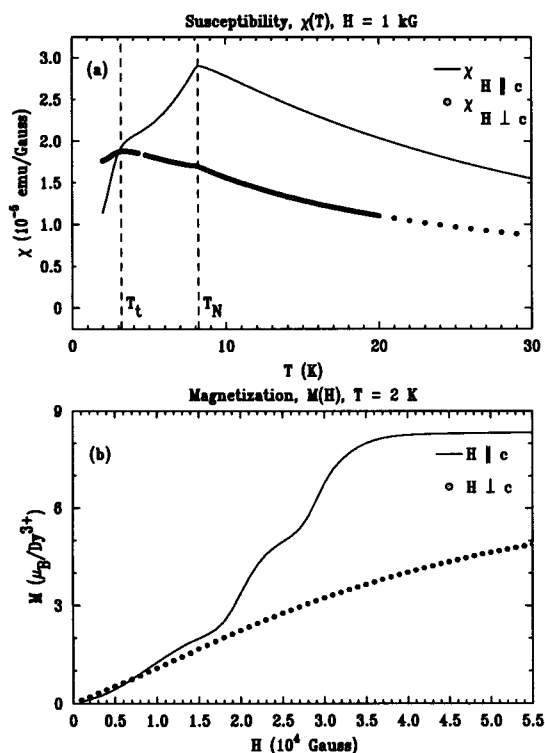


Fig. 1. (a) Susceptibility and (b) magnetization of DyNi<sub>2</sub>Ge<sub>2</sub> single crystal. The dashed vertical lines in (a) indicate the positions of the transition temperatures,  $T_N$  and  $T_t$ , respectively.

as mentioned above, the metamagnetic phase transitions in DyNi<sub>2</sub>Ge<sub>2</sub> may become sharper as the temperature is lowered below 2 K making this material another system for the study of metamagnetism.

### 3. NEUTRON DIFFRACTION MEASUREMENTS

For our neutron diffraction measurements, a single crystal of DyNi<sub>2</sub>Ge<sub>2</sub> was aligned in the [H H L] zone. At 11 K, well above  $T_N$  determined from the susceptibility data, scans along various symmetry directions in this zone showed only nuclear peaks consistent with the body centered tetragonal crystal structure (*i.e.*  $H+K+L = 2n$  where  $n$  is an integer) with lattice parameters  $a = 4.031 \pm 0.003$  Å and  $c = 9.776 \pm 0.004$  Å at this temperature. No significant variations of the lattice parameters with temperature were observed. Below  $T_N$ , magnetic satellite peaks corresponding to  $\tau_1 = (0 \ 0 \ \frac{3}{4})$  developed. The presence of weak magnetic satellites of  $(0 \ 0 \ L)$  associated with  $\tau_1$  indicated that there is a small component of the ordered moments in the basal plane perpendicular to the  $\hat{c}$  axis.

At 1.5 K, below the second transition at  $T_t$ , additional superlattice peaks associated with  $\tau_2 = (\frac{1}{2} \ \frac{1}{2} \ 0)$

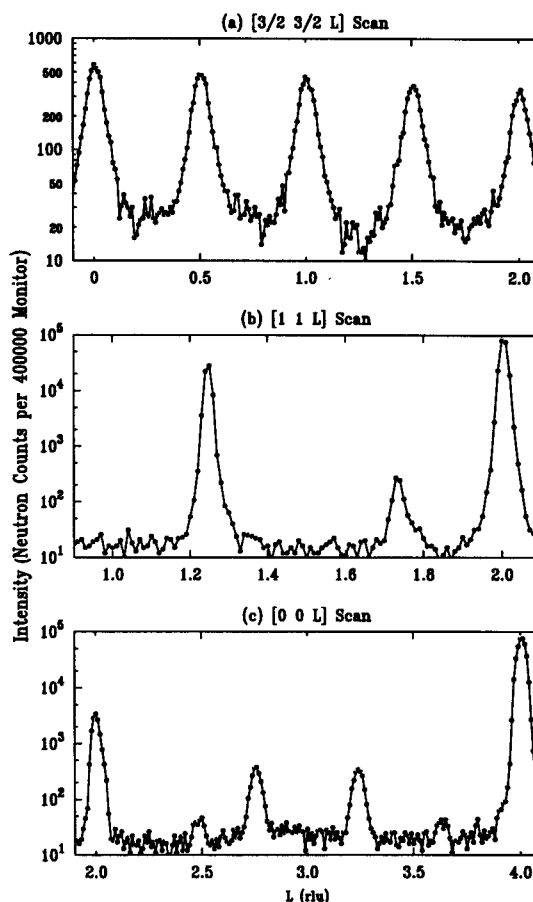


Fig. 2. Selected reciprocal lattice scans at 1.5 K in the [H H L] zone showing various magnetic peaks. (a)  $[\frac{3}{2} \ \frac{3}{2} \ L]$  scan, (b)  $[1 \ 1 \ L]$  scan and (c)  $[0 \ 0 \ L]$  scan. The small peaks at 2.5 and 3.6 in (c) are from a second grain in the sample. The  $\tau'_1$  satellites in the  $[0 \ 0 \ L]$  scan were too weak to be observed. Note that the intensities are shown on logarithmic scales.

and  $\tau_3 = (\frac{1}{2} \ \frac{1}{2} \ \frac{1}{2})$  emerged (see Fig. 2(a)). A third harmonic,  $\tau'_1 = (0 \ 0 \ \frac{1}{4})$ , related to  $\tau_1$  also developed indicating a squaring up of the structure.\* No other modulations in this zone were found. Again, the presence of relatively weak  $\tau$  and  $\tau'_1$  satellites of  $(0 \ 0 \ L)$  nuclear peaks imply a small component of the ordered moments in the basal plane. The magnetic unit cell of this structure consists of 16 chemical unit cells as implied by the simultaneous existence of  $\tau_1$  and  $\tau_2$ .

The integrated intensities of various magnetic Bragg peaks corresponding to  $(1 \ 1 \ 2)-\tau_1$ ,  $(1 \ 1 \ 2)-\tau'_1$ ,  $(1 \ 1 \ 2)+\tau_2$  and  $(2 \ 2 \ 2)-\tau_3$  are shown in Fig. 3 as a function

\* Here we mention that our definition of a propagation vector is made with respect to the center ( $\Gamma$ ) of the Brillouin zone (BZ) which has the full point group symmetry of the space group of the underlying crystal structure. Then the third harmonic of  $\tau_1 = (0 \ 0 \ \frac{3}{4})$  is  $3\tau_1$  which is  $\tau'_1 = (0 \ 0 \ \frac{1}{4})$  when reduced to the first BZ.

of temperature. The intensity of  $\tau_1$  satellite increases continuously from zero at  $T_N$  and has a small break at the lower phase transition at  $T_t$ . Below this temperature, magnetic peaks corresponding to  $\tau_2$  and  $\tau_3$  appear. Both  $\tau_2$  and  $\tau_3$  show very similar dependencies on temperature which suggests that these modulation vectors are related. The third harmonic becomes negligibly small above  $T_t$  indicating that the structure in this phase is essentially sinusoidal. As  $T_t$  is approached from above, the structure starts to square up giving rise to the harmonic.

The temperature dependence of these order parameters can be modeled by Brillouin type functions,  $B_J(|T - T_c|)$  where  $T_c$  is the transition temperature, shown by the solid lines in Fig. 3. In the case of the  $\tau_1$  order parameter,  $J = \frac{15}{2}$  was used whereas for  $\tau_2$  and  $\tau_3$ ,  $J = \frac{1}{2}$  was used. The transition temperatures thus obtained are  $T_N = 8.3 \pm 0.1$  K and  $T_t = 3.1 \pm 0.2$  K, in close agreement with those determined by susceptibility measurements. The fact that, below  $T_t$ , the  $\tau_2$  and  $\tau_3$  order parameters can be modeled by  $B_{J=\frac{1}{2}}$  suggests that the CEF ground state is a magnetic doublet. This is possible since  $\text{Dy}^{3+}$  is a Kramers ion. The CEF split  $J = \frac{15}{2}$  multiplet of  $\text{Dy}^{3+}$  will always be at least doubly degenerate in the absence of an external magnetic field.\* In the case of  $\text{DyNi}_2\text{Si}_2$  the magnetic entropy reaches  $\sim R \ln(10.7)$  at 30 K which suggests that the CEF level scheme contains at least five doublets within 50 K. [12] Due to the isostructural relationship and similar magnetic behavior with this compound a similar set of CEF levels in  $\text{DyNi}_2\text{Ge}_2$  seems feasible. In the temperature region below  $T_t$  only the low lying CEF levels are important due to thermal depopulation of the higher excited levels. Since more CEF eigenstates are likely to be involved above  $T_t$ , the temperature dependence of  $\tau_1$  is different than those of  $\tau_2$  and  $\tau_3$  below  $T_t$ .

Also, in the case of the  $\tau_1$  order parameter below  $T_t$ , there is a small enhancement of the intensity above that expected from the Brillouin function behavior. This is due to the Dy ions acquiring their full saturation value of  $10 \mu_B$  upon going through the transition at  $T_t$  from an AM structure above this temperature. If the structure remained AM below  $T_t$  then the break as shown in Fig. 3 is not expected.

The magnetically ordered phases of  $\text{DyNi}_2\text{Ge}_2$  are very similar to those found in the neighboring,

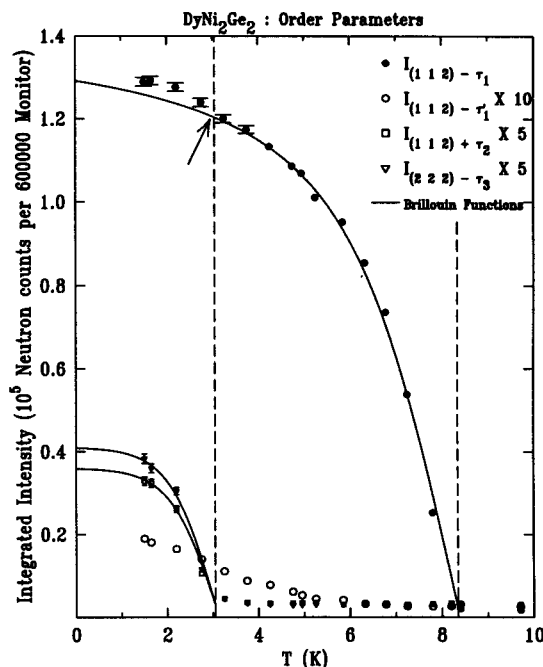


Fig. 3. Temperature dependence of various magnetic reflections measured by neutron diffraction ( $E_{\text{neutron}} = 14.7$  meV) on a single crystal. The arrow shows the break in the  $\tau_1'$  order parameter. The intensities of  $\tau_1'$  was multiplied by 10 and those of  $\tau_2$  and  $\tau_3$  satellites were multiplied by 5. Data were collected on raising the temperature. The vertical dashed lines locate the positions of the transition temperatures,  $T_N$  and  $T_t$ , respectively.

isostructural,  $\text{TbNi}_2\text{Ge}_2$  compound. [4] This material orders below 16.8 K ( $T_N$ ) in an AM *longitudinal* structure with propagation vector  $\tau \approx (0 \ 0 \ 0.758)$  whereas below 9.3 K ( $T_t$ ) the structure becomes equal moment (EM) *commensurate* with the same set of modulation vectors ( $\tau_1, \tau_1', \tau_2, \tau_3$ ) as was found in  $\text{DyNi}_2\text{Ge}_2$  below 3.2 K. The transition from the AM to an EM structure in  $\text{TbNi}_2\text{Ge}_2$  was also evidenced by the break and increase in intensity, of the  $\tau_1$  satellite at  $T_t$ . Unlike the Tb compound, where the ordered moments in both the phases are along the  $\hat{c}$  axis, there is a component of Dy moments in the basal plane, consistent with the susceptibility and low temperature magnetization measurements.

#### 4. MAGNETIC STRUCTURES AND DISCUSSION

Based on our results, and the isostructural relationship to  $\text{TbNi}_2\text{Ge}_2$ , a magnetic structure as shown in Fig. 4 for  $\text{DyNi}_2\text{Ge}_2$  below  $T_t = 3.1$  K seems feasible. In this EM phase all the Dy moments have their full saturation moment of  $10 \mu_B$  (consistent with the

\* The  $D_{J=\frac{15}{2}}$  manifold of  $\text{Dy}^{3+}$  ion reduces to even dimensional representations of the  $D_{4h}$  point group as follows:

$$D_{J=\frac{15}{2}} = 4\Gamma_6^- \oplus 4\Gamma_7^-$$

where  $\Gamma_6^-$  and  $\Gamma_7^-$  are the odd irreducible representations of the double group. See [18].

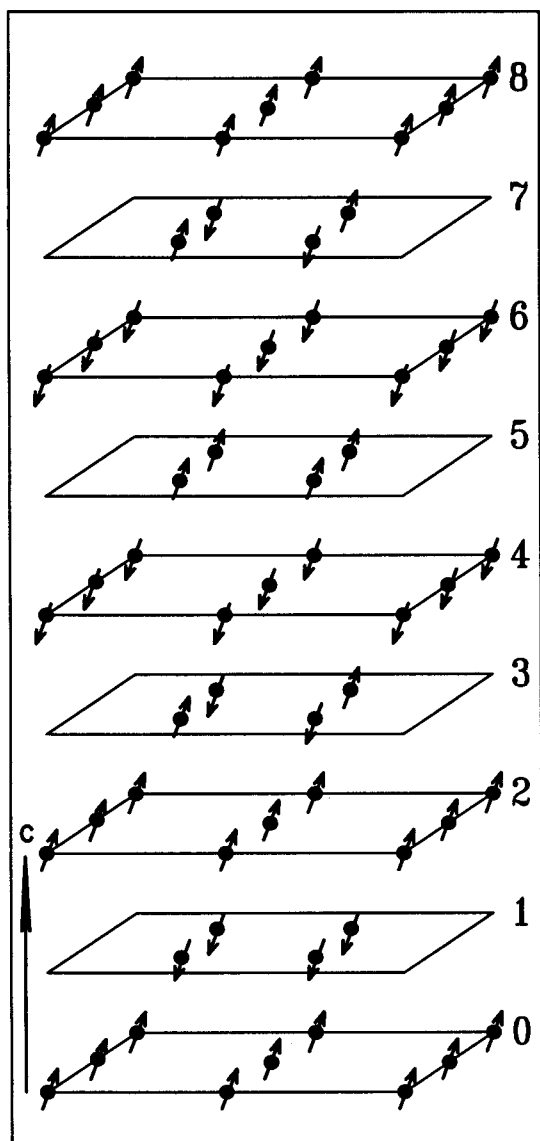


Fig. 4. The magnetic unit cell of  $\text{DyNi}_2\text{Ge}_2$  crystal below  $T_1 = 3.1$  K. The  $\uparrow$  ( $\downarrow$ ) represents the magnetic moment of Dy atoms (solid circles). Ni and Ge atoms have been omitted. The planes are numbered for reference.

Hund's rule ground state,  $^6H_{15/2}$ ) aligned at an angle  $\beta$  with respect to the  $\hat{c}$  axis. This structure consists of antiferromagnetically coupled, ferromagnetically ordered, Dy planes forming triplets (planes #0–#2 and #5–#7). Since two such neighboring triplets have opposite phases, the moments on planes #3 and #7 are 'frustrated' which can lead to antiferromagnetic ordering in these planes. This element of frustration can give rise to magnetic peak broadening below  $T_1$  as was observed to occur with high resolution XRES in  $\text{TbNi}_2\text{Ge}_2$  compound. [4] Due to extinction, shape and absorption effects in the neutron diffraction measure-

ments on a single crystal sample, a precise determination of the tilt angle  $\beta$  at this temperature could not be carried out. However, a rough estimate is  $\beta = 17^\circ \pm 6^\circ$ . Neutron diffraction from powdered single grains sample is clearly needed for a better determination of  $\beta$ . Due to the high neutron absorption cross section of Dy ( $\sigma_a = 940$  barns, see Ref. [19]), however, a better technique in this case is XRES on a single crystal sample for the moment direction determination as has been done in the  $\text{GdNi}_2\text{B}_2\text{C}$ ,  $\text{SmNi}_2\text{B}_2\text{C}$ ,  $\text{NdNi}_2\text{B}_2\text{C}$  and  $\text{TbNi}_2\text{Ge}_2$  compounds (see Refs [4, 11, 20]).

The magnetic structure above  $T_1$  but below  $T_N$  is a *sinusoidally* AM structure described by a single propagation vector,  $\tau_1$ , with no antiferromagnetic planes. The ordered moments are at an angle  $\beta$  from the  $\hat{c}$  axis. It is not clear if this  $\beta$  is different than that in the EM phase. The ordering scheme in  $\text{DyNi}_2\text{Ge}_2$  just described is like that in  $\text{DyNi}_2\text{Si}_2$ . [12, 14] The magnetic structure of  $\text{DyNi}_2\text{Si}_2$  below  $T_N = 6$  K but above  $T_1 = 3.7$  K is *sinusoidally* AM. Below  $T_1$ , the structure becomes EM *commensurate*. It is surprising, however, unlike the magnetic structures in  $\text{DyNi}_2\text{Ge}_2$ , the ordered moments in  $\text{DyNi}_2\text{Si}_2$  are aligned with the  $\hat{c}$  axis in both the phases although the magnetocrystalline anisotropies in both the materials are comparable. On the other hand,  $\text{TbNi}_2\text{Ge}_2$  and  $\text{TbNi}_2\text{Si}_2$  are strongly anisotropic with the ordered Tb moments strictly aligned with the  $\hat{c}$  axis. [4, 16]

The magnetic orderings in the three compounds  $\text{TbNi}_2\text{Ge}_2$ ,  $\text{TbNi}_2\text{Si}_2$  and  $\text{DyNi}_2\text{Si}_2$ , respectively, have two features in common. Below the respective ordering temperature,  $T_N$ , they all order in a *long period* AM structure. On further reducing the temperature the AM structure locks-into the lattice becoming EM *commensurate* at a lower transition temperature,  $T_1$ . Due to the similar magnetic behavior of  $\text{DyNi}_2\text{Ge}_2$ , in particular with that found in  $\text{TbNi}_2\text{Ge}_2$ , we expect the modulation vector below  $T_N$  to be slightly different from  $(0\ 0\ \frac{3}{4})$  found in the present neutron diffraction study, which implies a *longer period* of modulation as is the case in the other materials above  $T_1$  but below  $T_N$ . The high resolution available to XRES measurements should be utilized in order to determine  $\tau_1$  more precisely.

We point out that due to the four-fold symmetry of the trigonal basal plane the possibility of a spiral antiferromagnetic structure can not be ruled out. If, however, there is an in-plane easy direction of magnetization one way to search for it is to measure the angular dependence of dc magnetization (see Ref. [21]) within the basal plane. Similarly, one can try to determine  $\beta$  in the paramagnetic phase if the anisotropy is solely due to CEF effects. Such measurements to look

for any such in-plane easy direction as well as to determine  $\beta$  are planned. In addition, the difference between a collinear EM structure and a spiral one can also be determined with X-rays as well, using circularly polarized light (see Ref. [22, 23]).

Finally, the Néel transition temperature determined from our neutron diffraction measurements is in agreement with that from our susceptibility measurements and also with the one found in the earlier neutron work on a polycrystalline sample. [9] However, our results are inconsistent with the value of  $\tau_1 = (0\ 0\ 0.788)$  found by the previous workers. [9] The  $\tau_2$  and  $\tau_3$  satellites were not detected in the earlier work on a powder sample because they are very weak and Dy has a very large absorption cross section (see above). However, the large discrepancy of  $\tau_1$  can not be explained so easily. Although strains induced by grinding process can change the modulation, it is surprising that this could happen without significantly affecting  $T_N$ . An independent measurement using XRES can help resolve this discrepancy.

**Acknowledgements**—Ames Laboratory (U.S. Department of Energy) is operated by Iowa State University under Contract No. W-7405-Eng-82. This work was supported by the Director for Energy Research, Office of Basic Sciences. The work at Brookhaven National Laboratory was carried out under Contract No. DE-AC-0298CH10886, Division of Materials Science, U.S. Department of Energy.

## REFERENCES

1. Szytula, A. and Leciejewicz, J., *Handbook of Crystal Structures and Magnetic Properties of Rare Earth Intermetallics*, (CRC Press 1994), 114-192.
2. Canfield, P.C. and Fisk, Z., *Phil. Mag. B*, **56**, 1992, 1117.
3. Bud'ko, S.L. and Canfield, P.C., Unpublished.
4. Islam, Z., Detlefs, C., Goldman, A.I., Bud'ko, S.L., Canfield, P.C., Hill, J., Gibbs, D., Vogt, T. and Zheludev, A., *Phys. Rev. B*, **58**, 1998.
5. Islam, Z., Detlefs, C., Song, C., Goldman, A.I., Bud'ko, S.L., Canfield, P.C., Finkelstein, K., Hill, J.P. and Gibbs, D. Unpublished XRES studies.
6. Rieger, W. and Parthé, E., *Monatshefte für Chemie*, **100**, 1969, 444.
7. See the reference cited in A. Szytula, *Handbook of magnetic materials*, edited by K. H. J. Buschow, (Elsevier Science Publishers B.V., Amsterdam, The Netherlands, 1991), Vol. 6, Chap. 2, page 128-129.
8. See the reference cited in D. Gignoux, and D. Schmitt, *Handbook of magnetic materials*, edited by K. H. J. Buschow, (Elsevier Science Publishers B.V., Amsterdam, The Netherlands, 1997), Vol. 10, Chap. 2, page 369.
9. André, G., Bonville, P., Bourée, F., Bombik, A., Kolenda, M., Oleś, A., Sikora, W. and Szytula, A., *J. Alloys and Compounds*, **224**, 1996, 253.
10. Canfield, P.C., Cho, B.K., and Dennis, K., *Physics B*, **215**, 1995, 337.
11. Detlefs, C., Goldman, A.I., Stassis, C., Canfield, P.C., Cho, B.K., Hill, J.P. and Gibbs, D., *Phys. Rev. B*, **53**, 1996, 6355.
12. Garnier, A., Gignoux, D. and Schmitt, D., *J. Magn. Magn. Mat.*, **145**, 1995, 67.
13. Hashimoto, Y., Shigeoka, T., Iwata, N., Yoshizawa, H., Oohara, Y. and Nishi, M., *J. Magn. Magn. Mat.*, **140-144**, 1995, 903.
14. Ito, M., Deguchi, H., Takeda, K. and Hashimoto, Y., *J. Phys. Soc. Jap.*, **62**, 1993, 3019.
15. Shigeoka, T., Fujii, H., Nishi, M., Uwatoko, Y., Takabatake, T., Oguro, I., Motoya, K., Iwata, N. and Ito, Y., *J. Phys. Soc. Jap.*, **61**, 1992, 4559.
16. Blanco, J.A., Gignoux, D., Schmitt, D. and Vettier, C., *J. Magn. Magn. Mat.*, **97**, 1991, 4.
17. Bak, P. and von Boehm, J., *Phys. Rev. B*, **21**, 1985, 5297.
18. Koster, G.F., Dimmock, J.O., Wheeler, R.G. and Statz, H., *Properties of the Thirty-Two Point Groups*, (M.I.T. Press, Cambridge, Massachusetts, 1963), Character Table 40.
19. *International Tables for Crystallography*, edited by A. J. C. Wilson (Kluwer Academic Publishers Group, MA U.S.A., 1995), Vol. C, Chap. 4, Sec. 4.
20. Detlefs, C., Islam, A.H.M.Z., Goldman, A.I., Stassis, C., Canfield, P.C., Cho, B.K., Hill, J.P. and Gibbs, D., *Phys. Rev. B*, **55**, 1997, R680.
21. Canfield, P.C., Bud'ko, S.L., Cho, B.K., Lacerda, A., Farrell, D., Johnston-Halperin, E., Kalatsky, V.A. and Pokrovsky, V.L., *Phys. Rev. B*, **55**, 1997, 970.
22. Sutter, C., Grübel, G., Vettier, C., de Bergevin, F., Stunault, A., Gibbs, D. and Giles, C., *Phys. Rev. B*, **55**, 1997, 954.
23. Detlefs, C., Sanchez, J.-P., de Réotier, P.D., Kervanov, N. and Yaouanc, A., Private communications.